

## Central mode in hyper-Raman spectra of the quasi-one-dimensional hydrogen-bonded ferroelectric $\text{CsH}_2\text{PO}_4$

S. Shin, A. Ishida, T. Yamakami, T. Fujimura, and M. Ishigame

*Research Institute for Scientific Measurements, Tohoku University, 2-1-1 Katahira, Sendai, Miyagi 980, Japan*

(Received 22 September 1986)

A central mode of the quasi-one-dimensional hydrogen-bonded ferroelectric  $\text{CsH}_2\text{PO}_4$  (CDP) is found in the paraelectric phase by hyper-Raman scattering, for the first time. From the temperature and polarization dependences of the spectra, the observed central mode is assigned to be a soft mode which is related to the ferroelectric phase transition of CDP. From line-shape analysis, it is concluded that the central mode is caused by the polarization fluctuation of  $\text{PO}_4$  ions. Temperature dependences of the static susceptibility and the relaxation time are obtained from the intensity and the half-width of this central mode, respectively. Both temperature dependences are consistently explained by the quasi-one-dimensional Ising model.

### I. INTRODUCTION

Caesium dihydrogen phosphate  $\text{CsH}_2\text{PO}_4$  (CDP) is well known as a typical example of the hydrogen-bonded ferroelectrics.<sup>1-3</sup> The CDP is also known as one of a few one-dimensional ferroelectrics. The ferroelectric phase transition temperature  $T_c$  is around 150 K for CDP, while it increases around 270 K for the deuterated one ( $\text{CsD}_2\text{PO}_4$ ). This large isotope effect is a common property for the hydrogen-bonded compounds such as  $\text{KH}_2\text{PO}_4$  (KDP). In order to elucidate the role of proton tunneling for this isotope effect, the dynamics of phase transition for the hydrogen-bonded ferroelectrics has been studied so far by many researchers.<sup>4</sup>

However, because the precise mechanism of the phase transition in CDP has not been revealed, two different assertions seem to exist for the type of phase transition in CDP, depending on the experiments. One is the displacive-type mechanism coupled with the proton tunneling. This mechanism may qualitatively explain the large isotope effect of the CDP, assuming the existence of proton tunneling. On the contrary, the other is the ordinary order-disorder-type mechanism of polarized  $\text{PO}_4$  ions. This mechanism can well explain the Raman spectra of CDP.<sup>5-7</sup>

In paraelectric phase above  $T_c$ , the crystal structure of CDP (Refs. 8-11) is monoclinic with space group  $P2_1/m$  ( $C_{2h}^2$ ) which has the centrosymmetry. A proton occupies randomly one of the two equilibrium positions on a hydrogen bond which chains  $\text{PO}_4$  ions one dimensionally along  $b$  axis. In the ferroelectric phase below  $T_c$ , a proton occupies regularly one of the two positions accompanying displacements of the other heavy atoms. Then, the space group of crystal structure becomes  $P2_1$  ( $C_2^2$ ) in which the centrosymmetry is lost, causing a spontaneous polarization along the  $b$  axis.

Neutron scattering measurements<sup>12</sup> suggest that intra-chain correlations are strong compared with the inter-chain correlations in CDP. From this point of view, the dielectric properties of CDP have been considered on the basis of a quasi-one-dimensional Ising system by many au-

thors.<sup>2,3,13-16</sup> In connection with the relaxation process of the polarizations, the dynamic dielectric properties near the  $T_c$  are studied.<sup>3,15-17</sup> The results are also well explained by this model.

The soft mode in CDP, however, still has not been found in both paraelectric and ferroelectric phases, although the efforts to find a soft optic phonon in CDP have been made using Raman,<sup>5-7</sup> infrared,<sup>6</sup> and neutron<sup>12</sup> measurements.

Recently, the hyper-Raman scattering measurement is found to be a very useful tool to study the soft modes of the paraelectric phase in displacive-type ferroelectrics,<sup>18-22</sup> because these soft modes are active for hyper-Raman scattering as well as infrared absorption, while they are inactive for ordinary Raman scattering only when the crystal structure of the ferroelectrics has a centrosymmetry in the paraelectric phase. On the other hand, hyper-Raman scattering is also expected to be useful for the study of soft modes for the case of order-disorder-type ferroelectrics. As can be seen, the soft mode of this type in the paraelectric phase should be active for hyper-Raman scattering as well as infrared absorption. Furthermore, the soft mode in order-disorder-type ferroelectrics will be observed as a central mode by hyper-Raman scattering which is convenient to study the low-energy excitation spectra.<sup>23</sup> However, the study by means of hyper-Raman scattering is insufficient for the order-disorder-type ferroelectrics. The aim of this paper is to study the soft mode related to the phase transition of CDP by using the hyper-Raman scattering.

### II. EXPERIMENT

Single crystals of CDP were grown from an aqueous solution by the slow evaporation method at about 20°C.<sup>3</sup> The single crystals were cut into a rectangular shape in which the direction of each face was parallel to each crystallographic axis of  $c$ ,  $a'$ , and  $b$ , where  $a'$  is a pseudo-orthorhombic axis. All faces of this crystal were polished to give the optically flat surface. To define the polarization of hyper-Raman spectra, the orthogonal Cartesian

coordinate system  $X$ - $Y$ - $Z$  was used where  $X$ ,  $Y$ , and  $Z$  axes were taken parallel to the crystal axes  $c$ ,  $a'$ , and  $b$ , respectively.

An acoustic  $Q$ -switched Nd-YAG laser (YAG denotes yttrium aluminum garnet) was used as a light source. The wavelength was  $1.06 \mu\text{m}$  and the peak power of the pulses was about 20 kW at 1 kHz. The polarized laser beam with a single mode was focused into the sample by a lens of  $f=100 \text{ mm}$ . The light scattered at right angles was collected by a condenser lens through an analyzer. A double-grating monochromator was used with a slit width of  $100 \mu\text{m}$ , which gave a resolution of about  $3.9 \text{ cm}^{-1}$ . Since the intensity of the hyper-Raman scattering light was very weak, a gated photon counting system was used to reduce the dark count level of the photomultiplier by about  $1/10\,000$ . The remaining part of dark counts could be reduced to almost zero by the utilization of dark counts which were measured at an interval between two pulses of laser beam.

In order to measure the temperature dependence of spectra, a cryostat was used below 300 K and an electric furnace was used above 320 K. The temperature of the samples was kept constant within  $\pm 0.1 \text{ K}$  at the settled temperature by using a computer.

### III. RESULTS

Figure 1 shows the hyper-Raman spectra of CDP observed at temperatures 226, 298, and 393 K in the right-angle configuration  $X(ZZ)Y$ . The abscissa shows the fre-

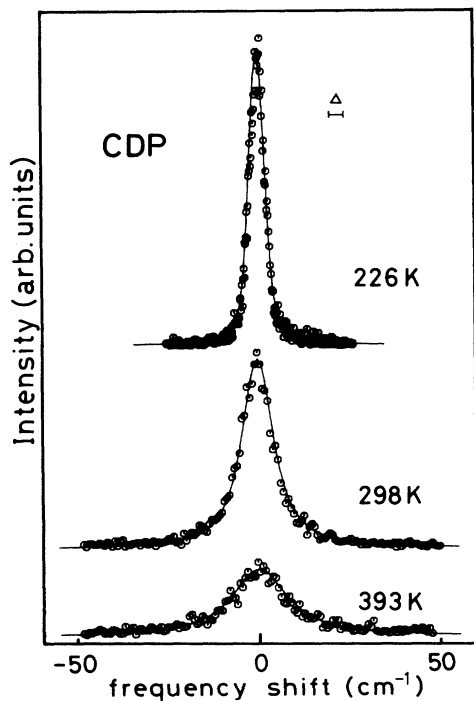


FIG. 1. The circles show the central mode in hyper-Raman spectra of CDP in the  $X(ZZ)Y$  configuration. The solid curves are the line shape of the Lorentzian convoluted by the slit function.

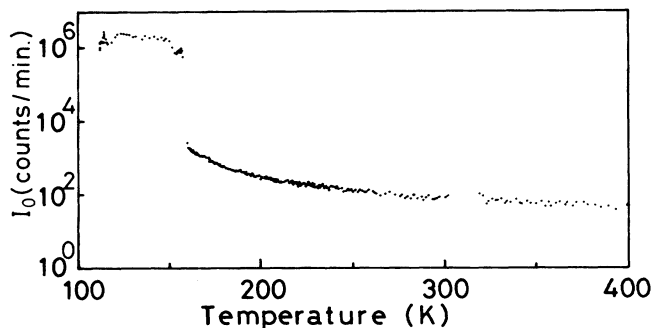


FIG. 2. Temperature dependence of the integrated intensity  $I_0$  of the central mode in CDP.

quency shift from  $2\omega_0$ , where  $\omega_0$  is the frequency of the incident laser beam. The spectra show clearly the central mode centered at  $0 \text{ cm}^{-1}$  with a linewidth wider than the resolution of  $\Delta=3.9 \text{ cm}^{-1}$ . Second-harmonic generation (hyper-Rayleigh) scattering which is the nonlinear elastic scattering is not seen in the spectra. If there were such a scattering, the linewidth of the spectrum should be the same as the resolution of  $3.9 \text{ cm}^{-1}$ . However, such a narrow scattering line is not found in this figure. This result is consistent with the fact that second-harmonic generation (SHG) of CDP is forbidden in the paraelectric phase because of the centrosymmetric crystal structure of the paraelectric phase of CDP.

In order to get the line shape of the spectra, we deconvolute the spectra by a slit function. Then, we find that the deconvoluted line shape is a Lorentzian. The convoluted Lorentzian line shape is in good accord with the experimental spectrum at each temperature, as shown by the solid curves in Fig. 1.

Comparing the three spectra in Fig. 1, it is seen that the

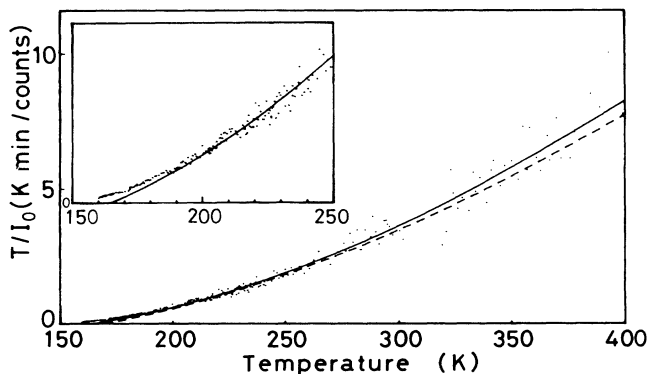


FIG. 3. Temperature dependence of  $T/I_0$  (dots) which is proportional to the inverse susceptibility  $1/\chi(0)$ . The solid curve is the calculated temperature dependence of  $1/\chi(0)$  which is fitted to  $T/I_0$  by the least-squares method using the quasi-one-dimensional Ising model. The dashed curve is the calculated temperature dependence of  $1/\chi(0)$ , using the quasi-one-dimensional transverse Ising model. The inset is the expansion of the temperature dependence near  $T_c$ .

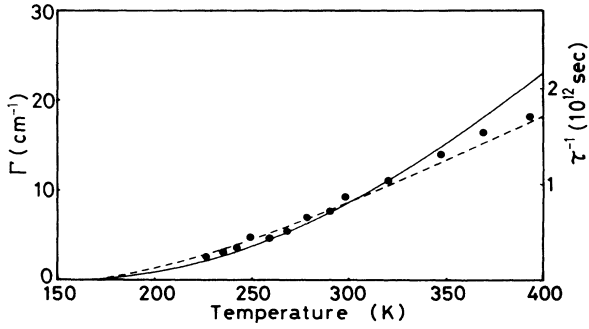


FIG. 4. Temperature dependence of the full half width  $\Gamma$  (solid circles) of the Lorentzian which corresponds to  $1/\pi c\tau$ . The solid curve is the calculated temperature dependence of  $1/\pi c\tau$  which is fitted to  $\Gamma$  by the least-squares method using the quasi-one-dimensional Ising model. The dashed curve is the calculated temperature dependence of  $1/\pi c\tau$ , using the quasi-one-dimensional transverse Ising model.

peak intensity of the central mode increases and its half width becomes narrow as the temperature decreases. In order to know the temperature dependence of the total intensity, we measure the intensity of the central mode using a wide slit width, which corresponds to the resolution of about  $60 \text{ cm}^{-1}$ , at temperatures from 100 to 400 K. The results are shown in Fig. 2. As seen from Fig. 2, the total intensity  $I_0$  increases gradually with decreasing temperatures. When the temperature becomes about 158 K, the total intensity increases rapidly and becomes almost constant below 157 K. Since the change of total intensity is too fast to be followed at a temperature range from 158 to 157 K, it is difficult to determine the order of this phase transition in CDP. The phase transition temperature  $T_c$ , however, is found to be about 157 K from the temperature dependence of  $I_0$ .

Figure 3 shows the temperature dependence of  $T/I_0$  in the paraelectric phase of CDP. From this figure, we can see that  $T/I_0$  becomes almost zero when the temperature is close to  $T_c \sim 157 \text{ K}$ . Figure 4 shows the temperature dependence of the full half width  $\Gamma$  of the Lorentzian which is obtained from the central mode by the deconvolution. It also approaches zero as the temperature goes to  $T_c$ . However, the half width of the Lorentzian below 220 K could not be obtained, because of the low resolution of the spectrometer of the system. In CDP, the spectral resolution was limited to about  $3.9 \text{ cm}^{-1}$  by the low intensity of the hyper-Raman scattering.

#### IV. DISCUSSIONS

As seen from Figs. 3 and 4, the intensity of the central mode diverges and the half width approaches zero, as the temperature approaches  $T_c$ . Furthermore, the central mode obtained by the configuration  $X(ZZ)Y$  (Ref. 24) has the same symmetry  $A_u$  as that of soft mode in CDP, which is derived by a group-theoretical consideration for the paraelectric phase.<sup>3</sup> From these experimental facts, it is confirmed that this central mode is a soft mode in CDP.

By the symmetry consideration,<sup>3,7,25</sup> it is known that the soft mode related to the phase transition of CDP has the symmetry of  $A_u$  in paraelectric phase and has the symmetry of  $A$  in ferroelectric phase. This means that the soft mode will be active for the infrared and the neutron measurements in both paraelectric and ferroelectric phases while it is active for the Raman measurement only in the ferroelectric phase. However, in infrared,<sup>6</sup> neutron,<sup>12</sup> and Raman<sup>5-7</sup> measurements, the soft optic mode has not yet been found. These facts suggest that the phase transition of CDP is not the ordinary displacive type.

As in the case of KDP, two possibilities of the phase transition mechanism are considered in CDP to understand the central mode obtained in this experiment. One mechanism is a displacive type, where the soft mode can be seen in the spectra as a damped harmonic oscillator in a very-low-frequency region. The other mechanism is an ordinary order-disorder type, which corresponds to the polarization fluctuation of  $\text{PO}_4$  ions, where the soft mode can be seen as a central peak. Then, a line-shape analysis of the obtained central mode is necessary to determine the phase transition type of CDP.

##### A. Line-shape analysis

First, we discuss the line shape of the central mode in order to clarify the phase transition mechanism in CDP. The intensity  $I(\omega)$  of hyper-Raman scattering is given by  $I(\omega) \sim n(\omega) \text{Im}\chi(\omega)$  for the anti-Stokes component and  $[n(\omega) + 1] \text{Im}\chi(\omega)$  for the Stokes component, where  $n(\omega)$  is the Bose-Einstein factor. This relation is also known for the intensity of ordinary Raman scattering spectra. From this relation, it is found that the line shape of  $I(\omega)$  is always derived from the frequency dependence of the imaginary part of susceptibility  $\chi(\omega)$ . In the low-frequency region ( $\hbar\omega \ll kT$ ),  $I(\omega)$  can be well approximated as  $I(\omega) \sim (kT/\hbar\omega) \text{Im}\chi(\omega)$ .

Assuming the order-disorder-type phase transition for CDP, the susceptibility  $\chi(\omega)$  in the frequency region of the central mode is given as  $\chi(\omega) = \chi(0)/(1 - i\omega\tau)$  by using a Debye model. Then, the frequency dependence of  $I(\omega)$  can be written as follows:

$$I(\omega) \sim \frac{kT}{\hbar} \chi(0) \frac{\tau}{1 + (\omega\tau)^2}. \quad (1)$$

This equation shows that the line shape of  $I(\omega)$  is Lorentzian except for the temperature factor.

On the contrary, for the displacive-type phase transition with the damped harmonic oscillator, the susceptibility  $\chi(\omega)$  is given by  $\chi(\omega) = \chi(0)\omega_0^2/(\omega_0^2 - \omega^2 - i\Gamma_0\omega)$ , where  $\omega_0$  is the frequency of the damped oscillator and  $\Gamma_0$  is the damping constant. In this case, the line shape of  $I(\omega)$  is given as follows:

$$I(\omega) \sim \frac{kT}{\hbar} \chi(0) \frac{\omega_0^2 \Gamma_0}{(\omega_0^2 - \omega^2)^2 + (\omega\Gamma_0)^2}. \quad (2)$$

The largest difference between Eqs. (1) and (2) is that the denominator of Eq. (1) has a second power of frequency shift while that of Eq. (2) has a fourth power of frequency shift. However, since the frequency dependence of  $I(\omega)$  in the latter case can be reduced to a Lorentzian type

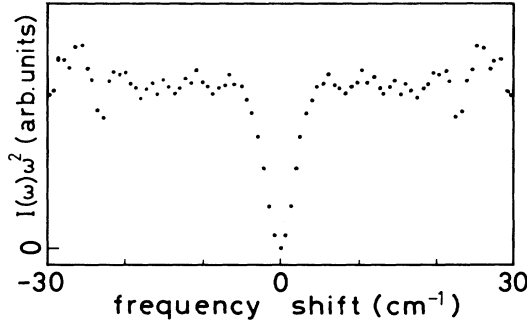


FIG. 5. Plot of  $I(\omega)\omega^2$  in which  $I(\omega)$  is the intensity symmetrized by the Stokes and anti-Stokes scattering spectra measured at 239 K.

in the low-frequency region, the frequency dependence of  $I(\omega)$  is very similar in both Eqs. (1) and (2) around the peak frequency region. Therefore, it is not easy to recognize which equation can well reproduce the experimental spectra by the comparison of the line shapes.

On the contrary, in the tail of the spectra in the high-frequency region, the difference between two line shapes is remarkable. If the line shape is given by a Lorentzian,  $I(\omega)\omega^2$  increases monotonously from the frequency shift  $\omega=0$   $\text{cm}^{-1}$  with increasing  $\omega$  and reaches a constant at the high-frequency region. On the other hand, if the line shape is given by a damped harmonic oscillator,  $I(\omega)\omega^2$  increases with increasing  $\omega$  and shows the maximum at  $\omega_0$ , and then decreases with increasing  $\omega$ . Thereupon, we try to plot  $I(\omega)\omega^2$  using the experimental spectra. The results are plotted in Fig. 5. As seen in Fig. 5,  $I(\omega)\omega^2$  increases with the increase of  $|\omega|$  and shows a constant in the frequency region above  $|\omega|=5$   $\text{cm}^{-1}$ . Therefore, it is considered that the line shape of the central mode in CDP is a Lorentzian within these experimental errors. From the line-shape analysis of the spectra described above, it is concluded that the mechanism of phase transition in CDP is an order-disorder type. In this case, the central mode is considered to be caused by the polarization fluctuation of  $\text{PO}_4$  ions.

The line-shape analysis described above seems to be very useful to elucidate the origin of hyperquasielastic light scattering. This line-shape analysis is also successfully applied to the hyperquasielastic light scattering spectra of liquids.<sup>26</sup> Hyper-Raman scattering measurement is believed to be a new experimental method to obtain an exact line shape of quasielastic light scattering spectra.

### B. Static susceptibility

Next, we discuss the temperature dependence of the static susceptibility of CDP based on the order-disorder-type phase transition mechanism.

Since the total intensity  $I_0$  is given by the integration of Eq. (1) over the whole frequency region, the following relation is derived:

$$\chi(0) \sim \frac{I_0}{kT}. \quad (3)$$

Consequently, the ordinate  $T/I_0$  in Fig. 3 should be proportional to  $1/\chi(0)$ . Equation (3) is also a well-known relation for ordinary Raman scattering.

The Hamiltonian for the quasi-one-dimension Ising model in an external electric field  $E_{ij}$  has the form<sup>27</sup>

$$H = - \sum_{i,j} \left[ J_{\parallel} S_{i+1,j} S_{ij} + \frac{1}{2} \sum_{m,n} J_{\perp mn} S_{ij} S_{i+m,j+n} + \mu S_{ij} E_{ij} \right],$$

where  $J_{\parallel}$  and  $J_{\perp}$  are the interchain intrachain coupling constants, respectively, and  $S_{ij} = \pm 1$  is the spin variable at the site  $i$  in the  $j$ th chain.  $m, n$  indicates the relative position of the interacting spins.  $\mu$  is the effective microscopic dipole moment. By using the mean-field approximation, the following equation:<sup>27,28</sup>

$$\chi(0) = \frac{N\beta\mu^2}{\exp(-2\beta J_{\parallel}) - \beta J_{\perp}}, \quad (4)$$

is obtained for  $T > T_c$ , where  $N$  is the number of spins in unit volume and  $\beta = 1/kT$ .

Since, using all of the experimental data above  $T_c$ , the parameter fitting in Eq. (4) was not successful by the least-squares method, only the experimental data above  $T_c + 20$  K were used to determine the parameters  $J_{\parallel}$  and  $J_{\perp}$ . Then, we can determine the values of the parameters so that the greater part of the experimental results  $I_0/T$  can be reproduced by the temperature dependence of  $\chi(0)$  calculated by this equation. The calculated temperature dependence of  $1/\chi(0)$  is shown by a solid curve in Fig. 3. In this figure, it is seen that experimental values  $T/I_0$  agree well with the calculated values  $1/\chi(0)$ . The evaluated values of fitting parameters  $J_{\parallel}$  and  $J_{\perp}$  are shown in Table I.

The temperature dependence of  $T/I_0$  in the vicinity of  $T_c$  could not be reproduced by using Eq. (4). Since, in the vicinity of  $T_c$ , values of  $T/I_0$  always exceed  $1/\chi(0)$  as shown by the inset in Fig. 3, it is considered that this deviation is not caused due to extra SHG, such as a defect-induced SHG. The reason for this deviation from the quasi-one-dimensional Ising model is not clear at present. However, this deviation has already been pointed out by a few workers.<sup>2,14,15</sup>

Static dielectric constant  $\epsilon_0$  of CDP has been discussed so far by many workers<sup>2,3,13-16</sup> using the quasi-one-dimensional Ising model. The reported experimental re-

TABLE I. Values of parameters  $J_{\parallel}$ ,  $J_{\perp}$ , and  $\tau_0$  used for the calculation by the quasi-one-dimensional Ising model, and values of parameters  $J_{\parallel}$ ,  $J_{\perp}$ , and  $\Omega$  used for the calculation by the quasi-one-dimensional transverse Ising model.

	Present work	Ref. 3	Ref. 14	Present work
$J_{\parallel}$ (K)	$273 \pm 10$	234	266	$302 \pm 24$
$J_{\perp}$ (K)	$6.0 \pm 0.5$	6.78	6.0	$9.3 \pm 6.7$
$\tau_0$ (s)	$5.7 \times 10^{-14}$	$1.9 \times 10^{-13}$	$6.7 \times 10^{-14}$	
$\Omega$ (K)				$135 \pm 38$

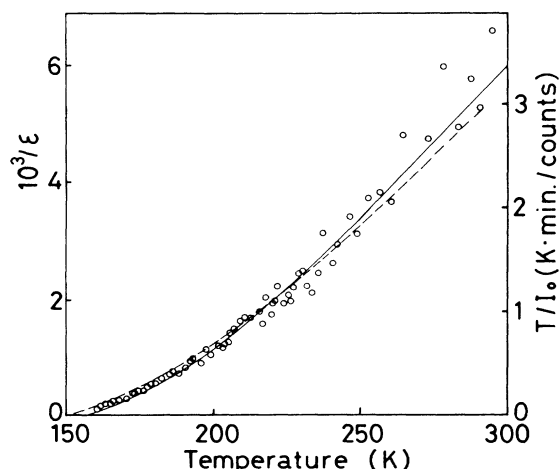


FIG. 6. Comparison between the inverse static dielectric constant  $1/\epsilon_0$  and  $T/I_0$  obtained by hyper-Raman scattering. The circles show  $T/I_0$ . The solid curve represents the temperature dependence of  $1/\epsilon_0$  reported by Deguchi *et al.* (Ref. 14). The dashed curve represents the temperature dependence of  $1/\epsilon_0$  reported by Kanda *et al.* (Ref. 3), where values of  $1/\epsilon_0$  are indicated using a reduced scale 0.62.

sults, however, are subtly different from each other and the parameters evaluated by the quasi-one-dimensional Ising model are also different from each other. Kanda *et al.*<sup>3</sup> reported that the temperature dependence of  $\epsilon_0$  is well explained by the quasi-one-dimensional Ising model. On the contrary, Blinc *et al.*<sup>2</sup> asserted that the temperature dependence of  $\epsilon_0$  can be reproduced by the quasi-one-dimensional Ising model only in a high-temperature region while, in the vicinity of  $T_c$ , the temperature dependence of  $\epsilon_0$  is reproduced better by the three-dimensional Ising model. From the behavior of this temperature dependence in  $\epsilon_0$ , they asserted that the three-dimensional correlation was dominant in a temperature region below  $T_c$  plus 3 K. On the other hand, Deguchi *et al.*<sup>14</sup> reported that the temperature dependence of the static dielectric constants in the vicinity of  $T_c$  can be described by neither the quasi-one-dimensional Ising model nor the three-dimensional Ising model.

Now,  $\epsilon_0$  and  $\chi(0)$  are considered to be almost numerically equal because  $\epsilon_0$  has a large value in the case of CDP. Therefore, the temperature dependence of  $\epsilon_0$  can be compared with the temperature dependence of the hyper-Raman scattering intensity directly. Figure 6 shows the comparison between  $1/\epsilon_0$  (Refs. 3 and 14) and  $T/I_0$ , which is obtained by hyper-Raman scattering. In this figure, it is found that the values of  $T/I_0$  measured in this experiment show the temperature dependence close to that of the  $1/\epsilon_0$  reported by Deguchi *et al.*<sup>14</sup> The evaluated values of parameters  $J_{\parallel}$  and  $J_{\perp}$  are in good accord with those reported by Deguchi *et al.*

### C. Relaxation time

Here, we discussed the temperature dependence of relaxation time  $\tau$  of CDP based on the order-disorder-type

phase transition mechanism. As shown in Fig. 1, the frequency dependence of the central mode is reproduced by a single Lorentzian at each temperature. This fact means that the distribution of relaxation times is not found in the central mode observed by hyper-Raman scattering. From the Cole-Cole plot of complex dielectric constants,<sup>3,17</sup> it is also shown that the distribution of relaxation time is hardly observed in frequency region from 1 to  $10^4$  MHz.

Using the quasi-one-dimensional Ising model,<sup>27</sup> the temperature dependence of relaxation time  $\tau$  is given by

$$\tau \sim \tau_0 kT \exp(2\beta J_{\parallel}) \chi(0), \quad (5)$$

where  $\tau_0$  is the relaxation time in the absence of the interaction between the dipoles. To estimate the value of  $\tau$  using Eq. (5), we use the values of parameters  $J_{\parallel}$  and  $J_{\perp}$  which are determined in Sec. IV B. Assuming that  $\tau_0$  is a constant parameter independent of the temperature, the observed temperature dependence of  $\Gamma$  is well reproduced by the solid curve in Fig. 4, where the solid curve is the temperature dependence of  $\Gamma = 1/\pi\tau$  calculated by Eq. (5). The value of  $\tau_0$  used in this calculation is  $5.7 \times 10^{-14}$  sec.

The inverse kinetic coefficient  $\tau/\chi(0)$  is shown in Fig. 7. The open circles are the values obtained by this experiment, which show an almost constant value in this temperature range. The solid curve is the calculated values  $\tau/\chi(0)$  using the following relation:

$$\frac{\tau}{\chi(0)} = \tau_0 kT \exp(2\beta J_{\parallel}). \quad (6)$$

In Fig. 7, it seems that the experimental results are also well reproduced by the calculated curve, though the calculated one shows little temperature dependence. Thus, from the discussions above, it is found that the temperature dependence of the inverse kinetic coefficient is also understood by the quasi-one-dimensional Ising model.

However, there remains a problem since  $\tau_0$  has no temperature dependence in this experiment. Detailed experimental studies of the temperature dependence of  $\tau_0$  seem to be few up to now. Assuming that the relaxation of polarization is caused by a thermally activated process, the temperature dependence of  $\tau_0$  can be easily derived as follows.<sup>29,30</sup>

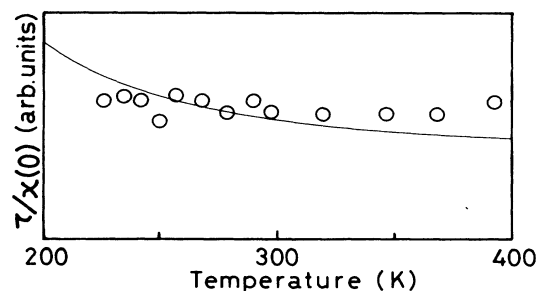


FIG. 7. Open circles show the temperature dependence of the inverse kinetic coefficient  $\tau/\chi(0)$ . Solid curve is  $\tau/\chi(0)$  calculated by the quasi-one-dimensional Ising model.

$$\tau_0 = \frac{h}{kT} \exp \left[ \frac{\Delta U}{kT} \right], \quad (7)$$

where  $\Delta U$  is an activation energy. This model also gives the short side limit of about  $10^{-12}$  sec to  $\tau_0$ . The evaluated value of  $\tau_0$  ( $5.7 \times 10^{-14}$  sec) in CDP, however, is shorter than this limit. Furthermore, if  $\tau_0$  has the temperature dependence of Eq. (7), the relaxation times calculated by Eq. (5) cannot reproduce the temperature dependence of the experimental results of the relaxation time of CDP.

For KDP crystal which is a hydrogen-bonded crystal similar to CDP, a constant value of  $\tau_0$  of about  $10^{-13}$  sec is used to explain the temperature dependence of the central mode which is observed by Raman scattering.<sup>31,32</sup> This fact is supported by Brillouin scattering of KDP.<sup>33</sup> On the contrary, in the case of  $\text{NaNO}_2$ ,<sup>29</sup> which is a typical example of order-disorder-type ferroelectrics, it is well known that  $\tau_0$  shows a temperature dependence which obeys Eq. (7). So far as we described above, a constant value of  $\tau_0$  is found only in the hydrogen-bonded ferroelectrics. However, it is not clear whether the constant  $\tau_0$  is a characteristic property of hydrogen-bonded ferroelectrics. Because there is a little study about the temperature dependence of  $\tau_0$ , hyper-Raman scattering must be carried out over a wide temperature range in order-disorder-type ferroelectrics other than CDP.

#### D. Analysis by quasi-one-dimensional transverse Ising model

Recently, a quasi-one-dimensional transverse Ising model is applied to the phase transition of CDP.<sup>34-36</sup> In this model, the role of the proton tunneling is taken into account in the phase transition mechanism. The Hamiltonian is given by

$$H = - \sum_{i,j} \left[ J_{\parallel} S_{i+1,j}^x S_{ij}^x + \frac{1}{2} \sum_{m,n} J_{\perp mn} S_{ij}^x S_{i+m,j+n}^x \right. \\ \left. + \Omega S_{ij}^z \right],$$

where  $\Omega$  is the tunneling energy. In CDP, the ratio of the proton tunneling energy to the intrachain interaction energy is very small ( $f = 2\Omega/J_{\parallel} \ll 1$ ). In this case, the theoretical calculation using this model gives a central-peak-type behavior in  $\chi(\omega)$ .<sup>34-36</sup> Therefore, it is worthwhile to try the analysis of the central mode observed by hyper-Raman scattering by using this model. By this model, static susceptibility  $\chi(0)$  and relaxation time  $\tau$  are given by the following equations:<sup>36</sup>

$$\chi(0) = \frac{\chi_{1D}(0)}{1 - J_{\perp} \chi_{1D}(0)}, \quad (8)$$

$$\tau = \frac{\tau_{1D}}{1 - J_{\perp} \chi_{1D}(0)}, \quad (9)$$

where

$$T_n = N^{-1} \sum \frac{f \cos(nka) + \cos[(n-1)ka]}{[1 + 2f \cos(ka) + f^2]^{1/2}} \tanh\left(\frac{1}{2}\beta E_k\right), \\ E_k = \frac{1}{2} J_{\parallel} [1 + 2f \cos(ka) + f^2]^{1/2},$$

$$k = \pm 2\pi m / Na, \quad m = 0, 1, \dots, N/2,$$

$$\chi_{1D}(0) = \frac{[1 - \exp(-\beta\Omega T_0)](1 + T_1 - T_0 T_2)}{\Omega T_0 (1 - T_1 + T_0 T_2)},$$

and

$$\tau_{1D} = \frac{\hbar \chi_{1D}(0)}{2T_0} \left[ 1 + \frac{2(T_1 - T_0^2 + T_1 T_{-1})}{f T_0} \right]^{1/2}.$$

Here,  $a$  is the distance between neighboring spins. According to the same way described in Sec. IV B, the values of parameters  $J_{\parallel}$ ,  $J_{\perp}$ , and  $\Omega$  are determined by the least-squares method so that the temperature dependences of  $1/\chi(0)$  and  $1/\pi c\tau$  calculated by Eqs. (8) and (9) can be reproduced by the experimental results  $T/I_0$  and  $\Gamma$  over the temperature range above  $T_c$  plus 20 K. The values of the parameters determined are given in the last column in Table I. The evaluated values of  $1/\chi(0)$  and  $\Gamma = 1/\pi c\tau$  are shown as dashed curves in Figs. 3 and 4. Both results seem to be very similar to the results of the ordinary quasi-one-dimensional Ising model. It is surprising that two kinds of Ising models used here give almost the same results for CDP though the physical mechanism included in the two models is quite different from each other. However, the deviation of the calculated  $\chi(0)$  from the experimental data in the vicinity of  $T_c$  could not be improved by this quasi-one-dimensional transverse Ising model.

The frequency dependence of  $\chi(\omega)$  by this model<sup>34,35</sup> is exactly given by a continued fraction representation of  $\omega$  which is derived by Plascak *et al.*<sup>35</sup> following Mori's formalism. In this case, the tail of the line shape in the high-frequency region may decay faster than that of the Lorentzian. This is contrary to the experimental fact that the line shape of the spectra shows clearly a Lorentzian. Therefore, we believe that the tunneling effect of the proton is not essential for the central mode of CDP observed by hyper-Raman scattering.

#### V. CONCLUSION

A central mode of the quasi-one-dimensional hydrogen-bonded ferroelectric  $\text{CsH}_2\text{PO}_4$  is found by hyper-Raman scattering. From the temperature and the polarization dependences of the spectra, the central mode is confirmed to be a soft mode of CDP. The line shape of this mode is determined to be a single Lorentzian type within these experimental errors. The mechanism for the phase transition is well explained by a relaxational Debye model for the order-disorder type, rather than a displacive-type model coupled with the proton tunneling. Hyper-Raman scattering intensity of the central mode is found to be related to the static susceptibility  $\chi(0)$ . The half width of the central mode is also related to the relaxation time  $\tau$ . The temperature dependence of  $\chi(0)$  is well explained by the quasi-one-dimensional Ising model. The temperature dependence of  $\tau$  is also well explained by the quasi-one-dimensional Ising model with a constant  $\tau_0$ .

However, two problems remain. First,  $\chi(0)$  are deviated from the values calculated by the quasi-one-dimensional Ising model in the vicinity of  $T_c$ . Second, we must consider the physical meaning of the constant  $\tau_0$  which has a short value. Since in the hyper-Raman spectra the soft mode will be obtained as a central mode in the order-disorder-type ferroelectrics, we believe that the hyper-Raman measurement is very useful to study the order-disorder-type ferroelectric as well as the displacive-type

one in which the soft mode will be obtained as a soft optic phonon.

#### ACKNOWLEDGMENTS

We are grateful to Dr. E. Kanda for his useful discussions. This work is partly supported by a Grant-in-Aid for Special Project Research from The Ministry of Education, Science and Culture, Japan.

- 
- <sup>1</sup>A. Levestik, R. Blinc, P. Kadaba, S. Cizikow, I. Levestik, and C. Filipic, *Solid State Commun.* **16**, 1339 (1975).  
<sup>2</sup>R. Blinc, B. Žekš, A. Levstik, C. Filipic, J. Slak, M. Burgar, I. Zupančič, L. A. Shuvalov, and A. I. Baranov, *Phys. Rev. Lett.* **43**, 231 (1979).  
<sup>3</sup>E. Kanda, A. Tamaki, and T. Fujimura, *J. Phys. C* **15**, 3401 (1982).  
<sup>4</sup>See, e.g., T. Matsubara, *Jpn. J. Appl. Phys.* **24**, Suppl. 24-2, 1 (1985).  
<sup>5</sup>M. Wada, A. Sawada, and Y. Ishibashi, *J. Phys. Soc. Jpn.* **47**, 1571 (1979).  
<sup>6</sup>B. Marchon and A. Novak, *J. Chem. Phys.* **78**, 2105 (1983).  
<sup>7</sup>M. Aoki, M. Kasahara, and I. Tatsuzaki, *J. Raman Spectrosc.* **15**, 97 (1984).  
<sup>8</sup>Y. Uesu and J. Kobayashi, *Phys. Status Solidi A* **34**, 475 (1976).  
<sup>9</sup>R. J. Nelmes and R. N. P. Choudhary, *Solid State Commun.* **26**, 823 (1978).  
<sup>10</sup>Y. Iwata, N. Koyano, and I. Shibuya, *J. Phys. Soc. Jpn.* **49**, 304 (1980).  
<sup>11</sup>K. Itoh, T. Hagiwara, and E. Nakamura, *J. Phys. Soc. Jpn.* **52**, 2626 (1983).  
<sup>12</sup>B. C. Frazer, D. Semmingsen, W. D. Ellenson, and G. Shirane, *Phys. Rev. B* **20**, 2745 (1979).  
<sup>13</sup>N. Yasuda, S. Fujimoto, M. Okamoto, H. Shimizu, K. Yoshino, and Y. Inuishi, *Phys. Rev. B* **20**, 2755 (1979).  
<sup>14</sup>K. Deguchi, E. Okaue, and E. Nakamura, *J. Phys. Soc. Jpn.* **51**, 3569 (1982).  
<sup>15</sup>A. Levestik, B. Žekš, I. Levestik, H. G. Unruh, G. Luther, and H. Roemer, *Phys. Rev. B* **27**, 5706 (1983).  
<sup>16</sup>E. B. Kryukova, *Fiz. Tverd. Tela (Leningrad)* **26**, 717 (1984) [*Sov. Phys—Solid State* **26**, 433 (1984)].  
<sup>17</sup>K. Deguchi, E. Nakamura, E. Okaue, and N. Aramaki, *J. Phys. Soc. Jpn.* **51**, 3575 (1982); K. Deguchi, E. Nakamura, and E. Okaue, *ibid.* **53**, 1160 (1984).  
<sup>18</sup>K. Inoue and N. Asai, *J. Phys. (Paris) Colloq.* **42**, C6-430 (1981).  
<sup>19</sup>H. Vogt, J. A. Sanjurjo, and G. Rossbroich, *Phys. Rev. B* **26**, 5904 (1982).  
<sup>20</sup>H. Vogt and H. Uwe, *Phys. Rev. B* **29**, 1030 (1984).  
<sup>21</sup>H. Vogt, *Jpn. J. Appl. Phys.* **24**, Suppl. 24-2, 112 (1985).  
<sup>22</sup>K. Inoue, *Jpn. J. Appl. Phys.* **24**, Suppl. 24-2, 107 (1985).  
<sup>23</sup>S. Shin and M. Ishigame, *Phys. Rev. B* **34**, 8875 (1986).  
<sup>24</sup>S. Shin and M. Ishigame (unpublished).  
<sup>25</sup>R. Blinc and B. Žekš, *Soft Modes in Ferroelectrics and Antiferroelectrics* (North-Holland, Amsterdam, 1974).  
<sup>26</sup>See, S. Shin and M. Ishigame, for hyper-Raman spectra of liquid CCl<sub>4</sub> (unpublished).  
<sup>27</sup>S. Žumer, *Phys. Rev. B* **21**, 1298 (1980).  
<sup>28</sup>A. V. de Carvalho and S. R. Salinas, *J. Phys. Soc. Jpn.* **44**, 238 (1978).  
<sup>29</sup>I. Hatta, *J. Phys. Soc. Jpn.* **28**, 1266 (1970).  
<sup>30</sup>W. P. Mason, *Phys. Rev.* **72**, 854 (1947).  
<sup>31</sup>Y. Tominaga, M. Tokunaga, and I. Tatsuzaki, *Jpn. J. Appl. Phys.* **24**, Suppl. 24-2, 917 (1985).  
<sup>32</sup>A. Sakai and T. Yagi, *Jpn. J. Appl. Phys.* **24**, Suppl. 24-2, 923 (1985).  
<sup>33</sup>M. Kasahara and Tatsuzaki, *J. Phys. Soc. Jpn.* **50**, 3972 (1981).  
<sup>34</sup>J. A. Plascak, A. S. T. Pieres, and F. C. Sá Barreto, *Solid State Commun.* **44**, 787 (1982).  
<sup>35</sup>J. A. Plascak, F. C. Sá Barreto, and A. S. T. Pieres, *Phys. Rev. B* **27**, 523 (1983).  
<sup>36</sup>S. Watarai and T. Mastubara, *J. Phys. Soc. Jpn.* **53**, 3648 (1984).